Charge transport mechanisms in microcrystalline silicon

S. J. Konezny,[a] M. N. Bussac,[b] and Libero Zuppiroli
Laboratoire d'Optoélectronique des Matériaux Moléculaires, STI-IMX-LOMM, Station 3, École Polytechnique Fédérale de Lausanne, CH-1015 Lausanne, Switzerland

(Received 22 October 2007; accepted 6 December 2007; published online 3 January 2008)

A heterogeneous charge transport model for microcrystalline silicon based on fluctuation-induced tunneling is presented that fits the low-temperature saturation observed in dark conductivity measurements and accounts for the film microstructure. Excellent agreement is found when the model is applied to data reported in the literature, particularly for highly crystalline samples, which produce the highest performance transistors. Values obtained for the three fitting parameters are consistent with typical measurements of microcrystalline silicon film morphology and the conduction band offset between amorphous and crystalline silicons. © *2008 American Institute of Physics*. [DOI: 10.1063/1.2828991]

With high mobilities and relatively low rates of light-induced degradation, hydrogenated microcrystalline silicon (μc-Si:H) may be used to improve upon the performance of commercially available transistors and photovoltaic cells based on amorphous silicon (*a*-Si). Since μc-Si:H can be prepared at low temperatures using the same fabrication infrastructure as *a*-Si:H, it also has potential as an active material for low-cost electronics applications requiring mechanical flexibility. The mechanisms responsible for charge transport in μc-Si:H, however, are not well understood.

The charge transport models for μc-Si:H that have been proposed to date are based on hopping, barrier-limited transport, or a combination of the two. These models do not account for the saturation in Arrhenius plots of the conductivity observed at low temperatures (see Fig. 1). Moreover, hopping transport cannot be responsible for measured field-effect mobilities on the order of 100 $cm^2/V\,s$.[1]

We present a heterogeneous model for microcrystalline silicon based on the framework of the fluctuation-induced tunneling mechanism proposed by Sheng[2] that predicts the correct temperature dependence of the conductivity and specifically takes into account the μc-Si:H thin-film microstructure. Important modifications to Sheng's model were made by Paschen *et al.* that extend its validity to low and high fields, yielding current densities with linear and Fowler-Nordheim behaviors, respectively.[3] The model presented in this letter includes those modifications proposed by Paschen *et al.* and some additional adaptations appropriate for the microstructure of μc-Si:H.

Fluctuation-induced tunneling conduction generally occurs in systems comprised of highly conductive regions separated by a relatively insulating medium. A representation of a single tunnel junction is depicted in Fig. 2(a) with an effective tunneling area A, a junction width w, and a zero-field barrier height eV_0. Since the electrons will tunnel between conductive regions at locations of closest approach, the effective tunneling cross section is generally small, resulting in a small junction capacitance. Under these conditions, temperature fluctuations of the conducting electrons will cause large voltage fluctuations across the junction and increase the tunneling probability by effectively lowering and narrowing the tunneling barrier. This process gives a temperature dependence to the tunneling conductivity, which would otherwise be temperature independent. At low temperatures, thermally activated fluctuation effects are negligible and the conductivity becomes effectively temperature independent. Figure 1 shows reported dark conductivity measurements for undoped μc-Si:H ranging below 170 K.[4–6] These data exhibit this characteristic low-temperature saturation.

A representation of the cross section of a typical μc-Si:H film is shown in Fig. 2(b). As depicted in the figure, an initial layer of pure amorphous silicon, the thickness of which depends on the deposition conditions, is deposited on the substrate before growth of the crystalline phase. As the thickness of the film increases, cone-shaped regions of packed silicon crystallites grow from these nucleation centers and increase in diameter until the surface reaches maximum crystallinity. Reports of crystallite and crystallite cluster sizes are typically 10–30 nm and 100–500 nm, respectively.[4,6,7] The microstructure can be characterized by conductive atomic force microscopy (AFM) measurements, which clearly show the large contrast in conductivity between the crystalline silicon (*c*-Si) crystallites and the amorphous medium.[8] Microcrystalline silicon therefore has both the microstructure and charge transport temperature depen-

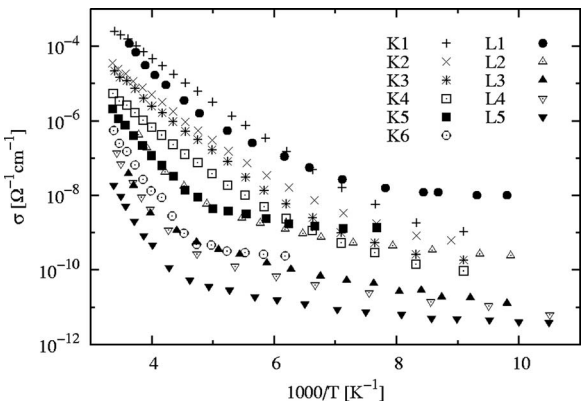

FIG. 1. Undoped microcrystalline silicon dark conductivity data as a function of temperature reported in Refs. 4–6.

[a]Electronic mail: sjkonezny@gmail.com.
[b]Permanent address: Centre de Physique Théorique, UMR-7644 du Centre National de la Recherche Scientifique, École Polytechnique, F-91128 Palaiseau Cedex, France.

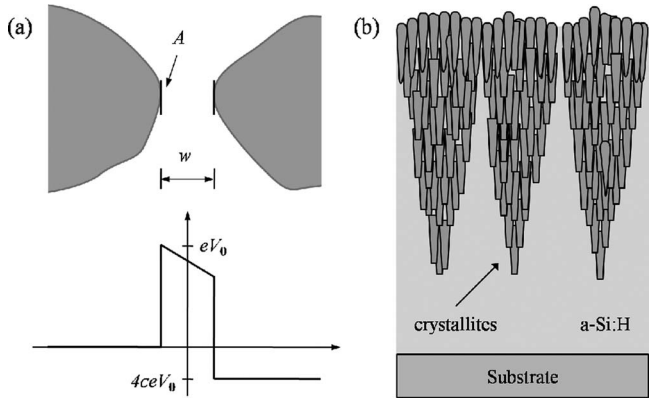

FIG. 2. (a) The location of closest approach between two highly conductive c-Si crystallites separated by a relatively insulating a-Si:H region with an effective tunneling area A, a junction width w, and a zero-field barrier height eV_0. The energy diagram of this junction in the presence of an electric field ϵ is represented below. (b) A cross-section representation of a typical μc-Si:H thin film showing crystallites and crystallite clusters embedded in amorphous silicon.

dence that are appropriate for fluctuation-induced tunneling.

Depending on the crystallinity of the μc-Si:H film surface, two types of tunnel junctions may be considered: the barriers created by the amorphous material between adjacent crystallites and the amorphous barriers between adjacent crystallite clusters. In both cases, the barrier height is expected to be equal to the conduction band offset between amorphous and crystalline silicon, though the offset may vary if, for example, the junction width is small enough to interfere with amorphous silicon hydrogenation. For high crystallinity samples, which have the highest conductivity and particular technological interest, transport can be described by a model based on the fluctuation-induced tunneling across a single junction.

The sketch in Fig. 3 is a simplified representation of the c-Si crystallites embedded in a-Si:H at the surface of a μc-Si:H thin film. The array of tunnel junctions at the regions of closest approach between crystallites is equivalent to the triangular resistor network shown on the right. The sheet conductance of a uniform resistor network is directly related to the conductance of a single resistor in the lattice. The fluctuation-induced conductivity $\bar{\sigma}$ of the film can therefore be expressed by

$$\bar{\sigma} = \frac{\gamma \bar{j} A}{tV}, \tag{1}$$

where t is the thickness of the sample, V is the applied voltage, γ is the sheet conductance proportionality constant, and $\bar{j}$ is the fluctuation-induced single junction current density defined below. We have calculated γ for various dimensions of the triangular network of Fig. 3 by applying a computational algorithm similar to the one used by Frank and Lobb.[9] As the dimensions of the network increase to values of typical device designs, γ converges to a value of 1.26. Other resistor network configurations can be explored, but the value of γ is not expected to vary enough to have an appreciable effect on the fitting parameters.[9]

Following the derivations of Paschen *et al.*,[3] the thermal fluctuation-induced current density $\bar{j}$ across a single junction is given by

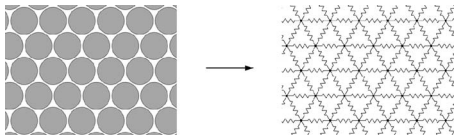

FIG. 3. A sketch of the c-Si crystallites embedded in a-Si:H at the surface of a μc-Si:H thin film and an equivalent resistor network. The tunnel junctions at the regions of closest approach between crystallites form a triangular resistor network.

$$\bar{j} = \sqrt{\frac{T_1}{\pi T}} \int_0^\infty dy j(y) [e^{-(T_1/T)(y-\epsilon)^2} - e^{-(T_1/T)(y+\epsilon)^2}], \tag{2}$$

where ϵ is the electric field in units of $4V_0/w$, the parameter T_1 is equal to $8AV_0^2\varepsilon/k_B w$, ε is the dielectric constant inside the junction, and $y=\epsilon+\epsilon_T$ is the sum of the electric and thermal fields. The current density across a single junction prior to thermal averaging $j(y)$ used in Eq. (2) is given by[3]

$$j(y) = \frac{me}{2\hbar^3}\left(\frac{eV_0}{\chi w \pi}\right)^2 \left\{ \frac{e^{-\chi w \xi}}{(\eta-\tau)\tau}[e^{\chi w(\eta-\tau)\alpha} - 1 - e^{-\chi w(\tau\alpha-\eta\alpha+4\tau y)} + e^{-4\chi w \eta y}] + \left[\frac{1}{\eta^2} + \frac{1}{(\eta+\tau)\tau}\right] \times \left(\frac{1-e^{-4\chi w \eta y}}{e^{\chi w \xi}}\right) + \left(\frac{1-e^{-4\chi w \tau y}}{\tau^2 e^{\chi w \tau \alpha}}\right) \right\}, \tag{3}$$

where m and e are the mass and charge of the electron, χ is equal to $\sqrt{2meV_0/\hbar^2}$, τ is equal to $eV_0/\chi w k_B T$, and three functions of y are defined as follows:

$$\xi(y) = \begin{cases} [1-(1-4y)^{3/2}]/3y, & y < 1/4 \\ 1/3y, & y \geq 1/4, \end{cases} \tag{4}$$

$$\eta(y) = \begin{cases} [1-(1-4y)^{1/2}]/2y, & y < 1/4 \\ 1/2y, & y \geq 1/4, \end{cases} \tag{5}$$

and

$$\alpha(y) = \begin{cases} 1, & y < \sqrt{3}/8 \\ \xi(y)/\eta(y), & y \geq \sqrt{3}/8. \end{cases} \tag{6}$$

Model fits for the data displayed in Fig. 1 are shown in Fig. 4. The fitting parameters and relevant device characteristics are given in Table I. Excellent agreement is obtained between the uniform single junction model and the reported experimental data, particularly for the high crystallinity samples reported by Kočka *et al.* [Fig. 4(a)]. Reports of the conduction band offset between a-Si:H and c-Si vary widely, but the fit values for the barrier height are distributed well within this range with an average value of 0.36 eV.[6,10,11] A distribution of barrier heights is to be expected if the concentration of impurities and the resulting shift in the Fermi energy vary from sample to sample. The junction widths are between 3.5 and 5.0 nm, values that are certainly plausible based on typical μc-Si:H film AFM images. The junction area is also consistent with TEM images, which show that the crystallites are needle shaped with the longest dimension perpendicular to the substrate.[7]

Liu *et al.* report lower crystallinity values for their samples (see Table I) and a slight deviation from theory and experiment is obtained near room temperature [Fig. 4(b)]. Such a deviation is expected for low crystallinity samples since the surface less resembles a uniform resistor network

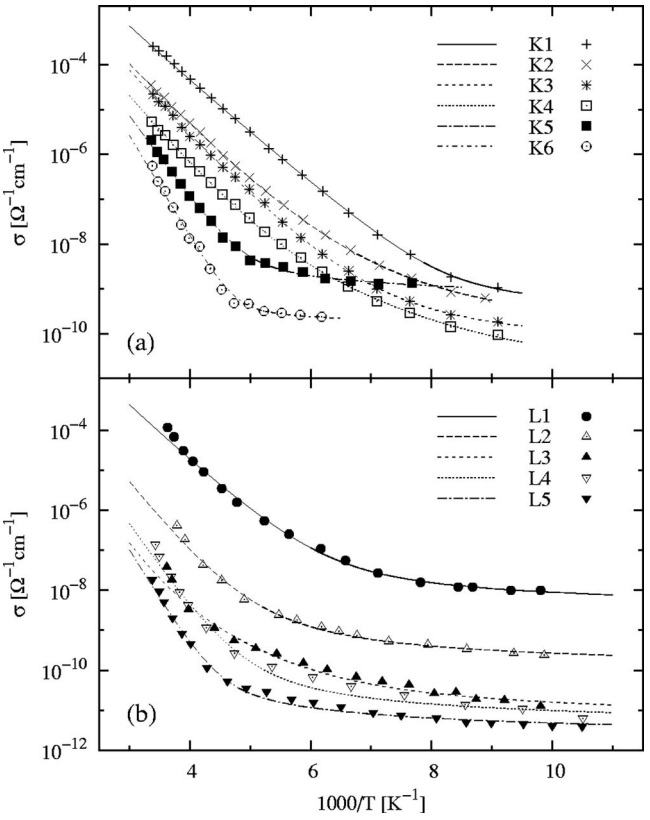

FIG. 4. Model fits for experimental data reported by (a) Kočka *et al.* and (b) Liu *et al.* Fitting parameters are given in Table I.

and a second type of barrier, the junction between crystallite clusters, becomes distinguishable from the crystallite-crystallite barriers. We applied a two junction model similar to the approach outlined in Ref. 13, with the exception that all six double junction parameters are fit, and the deviation vanishes. Though additional parameters are needed for an optimum fit at low crystallinity, the improved results suggest that the fluctuation-induced tunneling mechanism is still valid.

A benefit of such a multijunction model is that it allows for more accurate treatment of the heterogeneous nature of μc-Si:H. In general, when a hierarchy of barrier levels is considered,[13] only the disorder level with the lowest barriers, i.e., the most crystalline regions of the sample, significantly contributes to the film conductivity. In the case of a device with a top-contact geometry, for example, the incubation layer is expected to play a negligible role due to its considerably larger resistivity. The model and results presented in this letter show that for highly crystalline films, which yield the highest performance transistors, transport can be accurately described by a single fluctuation-induced tunneling junction.

TABLE I. Experimental data references, reported μc-Si:H film thickness t and crystallinity χ_c, and model fit parameters used for Fig. 4.

	References	t (μm)[a]	χ_c (%)	eV_0 (eV)	w (Å)	A (nm^2)
K1	4	4.7	87	0.20	49.2	131
K2	5	1.8		0.28	44.1	45.3
K3	4	2.2	88	0.28	45.3	54.5
K4	4	1.1	88	0.34	43.9	28.6
K5	4	2.75		0.32	37.6	74.9
K6	4	0.6	84	0.41	39.0	155
L1	6	0.7	79	0.26	40.3	61.0
L2	6	0.7	77	0.39	37.7	30.7
L3	6	0.7	57	0.53	35.9	14.6
L4	6	0.7	75	0.45	39.8	29.6
L5	6	0.7	68	0.48	39.7	35.3

[a]Reference 12.

We thank C. Ballif, E. Vallat-Sauvain, and N. Wyrsch for productive discussions and the Swiss National Science Foundation (Project No. 200020-113254) and the Interuniversity Center of Micro and Nanotechnology (CIMENT) project on flexible electronics for financial support.

[1]C. H. Lee, A. Sazonov, A. Nathan, and J. Robertson, Appl. Phys. Lett. **89**, 252101 (2006).
[2]P. Sheng, Phys. Rev. B **21**, 2180 (1980).
[3]S. Paschen, M. N. Bussac, L. Zuppiroli, E. Minder, and B. Hilti, J. Appl. Phys. **78**, 3230 (1995).
[4]J. Kočka, A. Fejfar, V. Vorliček, H. Stuchlíková, and J. Stuchlík, *Amorphous and Heterogeneous Silicon Thin Films: Fundamentals to Devices-1999*, Materials Research Society Symposia Proceedings Vol. 557 (Materials Research Society, San Francisco, 1999), p. 483.
[5]J. Kočka, A. Fejfar, P. Fojtík, K. Luterová, I. Pelant, B. Rezek, H. Stuchlíková, J. Stuchlík, and V. Švrček, Sol. Energy Mater. Sol. Cells **66**, 61 (2001).
[6]F. Liu, M. Zhu, Y. Feng, Y. Han, J. Liu, S. Kasouit, and R. Vanderhaghen, J. Non-Cryst. Solids **299**, 385 (2002).
[7]E. Vallat-Sauvain, A. Shah, and J. Bailat, in *Thin Film Solar Cells*, edited by J. Poortmans and V. I. Arkhipov (Wiley, New York, 2006), p. 133.
[8]T. Mates, P. C. P. Bronsveld, A. Fejfar, B. Rezek, J. Kočka, J. K. Rath, and R. E. I. Schropp, J. Non-Cryst. Solids **352**, 1011 (2006).
[9]D. J. Frank and C. J. Lobb, Phys. Rev. B **37**, 302 (1988).
[10]G. Lucovsky, C. Wang, and Y. L. Chen, J. Vac. Sci. Technol. A **10**, 2025 (1992).
[11]F. Evangelisti, J. Non-Cryst. Solids **77-78**, 969 (1985).
[12]Film thicknesses of Ref. 6 samples are based on private communication.
[13]S. J. Konezny, M. N. Bussac, A. Geiser, and L. Zuppiroli, Proc. SPIE **6658**, 66580 (2007).